



WMAP3 Results and the Observability of Reionization at Redshifted 21cm

G. Mellema^{1,2*}, I. T. Iliev³, Ue-Li Pen³, and Paul R. Shapiro⁴

¹ ASTRON, P.O. Box 2, NL-7990 AA Dwingeloo, The Netherlands

² Sterrewacht Leiden, P.O. Box 9513, NL-2300 RA Leiden, The Netherlands

³ Canadian Institute for Theoretical Astrophysics, University of Toronto, 60 St. George Street, Toronto, ON M5S 3H8, Canada

⁴ Department of Astronomy, University of Texas, Austin, TX 78712-1083, USA

Abstract. We present results from two new large scale simulations of the Epoch of Reionization based on the new 3 year WMAP cosmological parameters. For these parameters the peak of the reionization process falls below redshift 10, and hence above frequencies of 140 MHz, which should make it more easily observable with an instrument such as SKA. We present some global reionization history parameters and redshifted 21cm observables.

1. Introduction

One of the key science goals of SKA is to probe the end of the Dark Ages, when the first sources started to reionize the hydrogen in the intergalactic medium (IGM). This will be done by studying the redshifted 21cm radiation from neutral hydrogen at that era. Finding redshifted 21cm radiation from the epoch of reionization is also one of the key projects of LOFAR¹, as well as the main science goal of 21CMA (formerly PAST) and MWA². As a consequence there has been great activity in trying to understand the process of reionization, and to explore the possibilities of the upcoming observations to detect and characterize the redshifted 21cm emission. See the review in Furlanetto et al. (2006) for an overview of recent developments, and Furlanetto & Briggs (2004) for a review from an SKA perspective.

Large volumes need to be simulated both to be relevant for the planned observations (for example, one LOFAR station beam will be 2° across, corresponding to an physical scale of around 200/h Mpc comoving at a redshift of 9), to be able capture the biggest HII regions (from clustered sources), as well as to get away from cosmic variance (Barkana & Loeb 2004). At this time in the evolution of the universe most collapsed objects (galaxies or proto-galaxies) will be of low mass, and it is therefore expected that the source population responsible for reionization was dominated by these (proto-)dwarf galaxies. To resolve these in a large volume requires a mass resolution similar to that of the largest N-body simulation done to date (Millennium simulation³ Springel et al. 2005), or even

better. Even if this can be achieved, calculating the transfer of ionizing photons from the millions of sources present in such a volume will form the next computational hurdle.

Using a combination of two very computationally efficient tools, PMFAST (Merz et al. 2005) for structure formation, and C²-Ray (Mellema et al. 2006a) for radiative transfer, we have been able to construct a set of numerical models which captures the effects of large scale reionization. More details can be found in Iliev et al. (2006a), Mellema et al. (2006b), and Iliev et al. (2006b). Here we would like to present the results of two of our more recent simulations, which use the new WMAP3 cosmological parameters.

2. Simulation parameters

In our naming scheme the simulations presented here are known as f250-WMAP3 and f250C-WMAP3. They use the results of a PMFAST cosmological structure formation simulation in a volume of 100/h Mpc (comoving) across, with the new three year WMAP cosmological parameters (Spergel et al. 2006): $(\Omega_m, \Omega_\Lambda, \Omega_b, h, \sigma_8, n_s) = (0.24, 0.76, 0.042, 0.73, 0.74, 0.951)$, where Ω_m , Ω_Λ , and Ω_b are the total matter, vacuum, and baryonic densities in units of the critical density, h is the Hubble constant in units of 100 km s⁻¹Mpc⁻¹, σ_8 is the standard deviation of linear density fluctuations at present on the scale of 8/h Mpc, and n_s is the index of the primordial power spectrum. The PMFAST simulation uses a grid of 3248³ with 1624³ particles. The radiative transfer is done on a reduced grid of 203³. The other details of the simulation are as given in Iliev et al. (2006a) and Mellema et al. (2006b).

With the mass resolution used, the smallest collapsed objects we can accurately find have a mass of $2.1 \times 10^9 M_\odot$. For a halo to be able to collapse and form stars, its baryons need to be able to radiatively cool. Halos with masses higher than $\sim 10^8 M_\odot$ should be able to cool

* current address: Stockholm Observatory, AlbaNova University Centre, SE-10691 Stockholm, Sweden

¹ <http://www.lofar.org>

² <http://www.haystack.mit.edu/ast/arrays/mwa/>

³ Note that the parameters of the Millennium Simulation itself give it a mass resolution too low to be useful for studying reionization.

Table 1. Global reionization history results.

Model	$z_{50\%}$	z_{overlap}	τ_{es}
f250_WMAP3	8.9	7.5	0.086
f250C_WMAP3	8.4	6.5	0.080
f250_WMAP1	11.7	9.3	0.121
f250C_WMAP1	11.0	8.2	0.107

through atomic cooling, lower mass halos (mini-halos) would need to cool through molecular hydrogen. Since hot stars produce large amounts of photons in the Lyman-Werner bands, capable of destroying H_2 , a reasonable assumption is that during reionization mini-halos, although ubiquitous, are not contributing to the production of ionizing photons. This leaves only the halos with masses above $\sim 10^8 M_\odot$ as sources. However, as shown in Iliev et al. (2006b), the self-regulating character of reionization makes that halos below $\sim 10^9 M_\odot$ (the Jeans-mass filtering limit) are only important during the early stages of reionization. The later stages of large scale reionization are dominated by the more massive halos, which are the ones we are resolving here.

For each halo we assume a photon efficiency number of f_γ of 250. This overall efficiency is the product of the escape efficiency of ionizing photons from the halo f_{esc} , the star formation efficiency of the halo f_* and the typical number of photons produced per baryon for the stellar population N_i : $f_\gamma = f_{\text{esc}} f_* N_i$. For escape and star formation efficiencies of 10%, a value of 250 corresponds to a slightly top heavy initial mass function (IMF), for higher values of f_{esc} and f_* it corresponds to a standard Salpeter-type IMF.

For f250C we add the effect of redshift dependent subgrid clumping which was derived from a separate PMFAST calculation, see Mellema et al. (2006b) and Iliev et al. (2006b) for more information on how this was done. Since ionization will reduce gas clumping, the two simulations, f250 without and f250C with subgrid clumping, bracket its effect.

3. Global Reionization History

Table 1 summarizes the basic results on the global reionization history. For comparison it also lists the values of the corresponding simulations that used the first year WMAP cosmology. One sees that with the new WMAP results, reionization shifts to substantially lower redshifts. This mostly due to the lower slope of the power spectrum of initial fluctuations (n_s), and the lower amplitude of these fluctuations (σ_8). This shifts structure formation to lower redshifts and delays the entire reionization process. Alvarez et al. (2006) estimated that corresponding reionization histories in WMAP1 and WMAP3 cosmologies should be related by $(1+z_1)/(1+z_3) \approx 1.4$. We find a similar relation in the range 1.3 to 1.4 in the simulations.

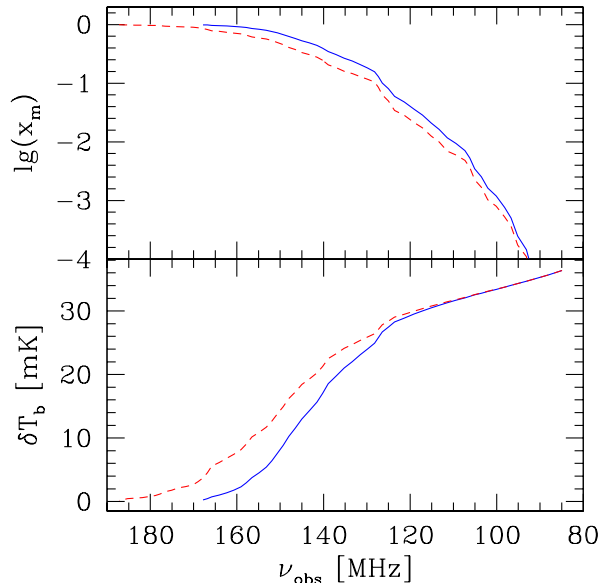


Fig. 1. Evolution of (top) the mean mass ionized fraction, x_m , and (bottom) the mean differential brightness temperature, δT_b , both as a functions of frequency for f250 (solid, blue), and f250C (short-dashed, red).

The WMAP3 value for τ_{es} is given as 0.09 ± 0.03 (Spergel et al. 2006), so both simulations fit this value. Interestingly, Spergel et al. (2006) quote a value of 11 as the redshift for instantaneous reionization, which is even substantially above the redshift of 50% ionization we found, illustrating that parameters derived from simple reionization models do not give accurate descriptions of complex reionization histories. Since both our simulations end near redshift 7, these results are easier to reconcile with the observations of high redshift quasars, which point to an end of reionization around a redshift of 6.5 (Fan et al. 2006).

The top panel of Fig. 1 shows the evolution of the mean, mass-weighted ionization fraction in both simulations, plotted against frequency. As in the previous simulations, the peak of the fluctuations happens at the point where 50 % of the mass ionized. For a resolution of $1'$ and 10 kHz the value of these fluctuations is found to be about 11 mK.

4. The 21cm signal

If the spin temperature of the neutral IGM (T_S) is substantially above the cosmic microwave background (CMB) temperature (T_{CMB}), the 21cm differential brightness temperature can be derived to be

$$\delta T_b \approx (28\text{mK}) \left(\frac{1+z}{10} \right)^{1/2} (1+\delta), \quad (1)$$

depending only on the redshift z , and the mean neutral hydrogen density in units of the mean density of hydrogen

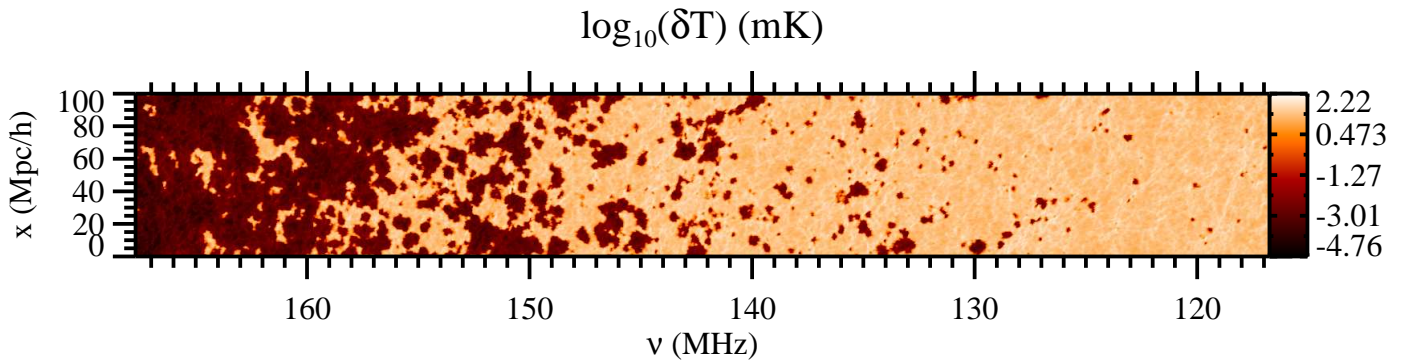


Fig. 2. Position-frequency slice for f250_WMAP3. The spatial scale is in comoving units. These slices illustrate the large-scale geometry of reionization seen at 21-cm and the significant local variations in reionization history. Observationally it corresponds to a slice through a high resolution image-cube.

at redshift z , $1 + \delta = \rho_{\text{HI}}/\langle\rho_H\rangle$ (Mellema et al. 2006b). Under this assumption it is trivial to calculate the differential brightness temperature of the redshifted 21cm signal. During reionization the overall gas temperature of the IGM (T_k) is expected to be above the CMB temperature due to heating by shocks, and X-rays, and the first sources will provide sufficient amounts of Ly α photons to couple T_S to T_k (Ciardi & Madau 2003). We note however that locally this may not always be true, especially during the early period of reionization, and it would be useful to check this assumption against detailed simulations.

The simulations give us the neutral hydrogen fraction and density at a number of redshifts. From this we construct the 21cm signal using Eq. 1. In Fig. 2 we show a cut through the simulation volume of f250_WMAP3 where we have taken into account the redshift evolution along the line of sight, and the redshift distortions due to the velocity field. To avoid passing several times over the same structures in our periodic volume, we took lines of sight going through the volume at an angle. This slice corresponds to a slice along the frequency direction through an idealized radio image cube. This representation shows clearly the progress of reionization from high to low redshift, and its patchiness and large variations with position. The neutral areas also show the effect of the density variations in the IGM, basically the cosmic web.

This slice can be compared to the one presented for simulation f250_WMAP1 in the lower panel of Fig. 4 in Mellema et al. (2006b) (note that the axis there is redshift, not frequency). The results look similar, except for the shift in redshift. The difference in the results is entirely due to the change in cosmology since all other parameters in the calculation are the same. This figure shows what was already pointed out above, in the WMAP3 cosmology, reionization is moved to lower redshifts. This difference (if true) implies that SKA and the other upcoming low frequency experiments will have a much better chance of observing the redshifted 21cm radiation from the epoch of reionization. The main signal will be at frequencies well above the FM-band (a major source of RFI), the iono-

sphere is more well-behaved and the galactic foreground is weaker at higher frequencies.

Our simulations have an intrinsic resolution of approximately 15'' and 30 kHz per cell. SKA is not expected to achieve this spatial resolution at the sensitivity needed to detect the faint signal of reionization, but its frequency resolution may actually be better. Assuming a maximum baseline of approximately 6 km, the resolution of SKA at a wavelength of 2m would be $\sim 1'$. Typically, the frequency resolution is of the order 1 kHz. Being an interferometer, SKA's actual beam shape will be complicated. For the images we present here, we use a compensated Gaussian, an analytical function with a mean value of zero, which mimics the effects of the missing zero spacings⁴. Since the 21cm signal is a smoothly varying signal in the sky, there is little point in trying to construct a Gaussian beam pattern which is more appropriate for point sources.

In Fig. 3 we show two images, from the redshifts of 50% and 90% ionization. The flat areas are the HII regions, but even the peaks show considerable structure, reflecting the underlying density field.

In Fig. 4 we show the frequency dependence along several adjacent lines of sight. This is basically a set of cuts through Fig. 2, and so includes redshift distortions due to peculiar motions. It shows the data at the resolution of the simulation.

5. Conclusions

We presented the results of new reionization simulations based on the 3 year WMAP cosmological parameters. These simulations show that in this cosmology, reionization happened considerably later, and would have observational signatures in the redshifted 21cm line between 120 and 180 MHz. Apart from this important shift in redshift, the results of the simulations are quite similar to those in Iliev et al. (2006a) and Mellema et al. (2006b), and the scaling relation of Alvarez et al. (2006),

⁴ For realistic images a proper beam shape should be used however.

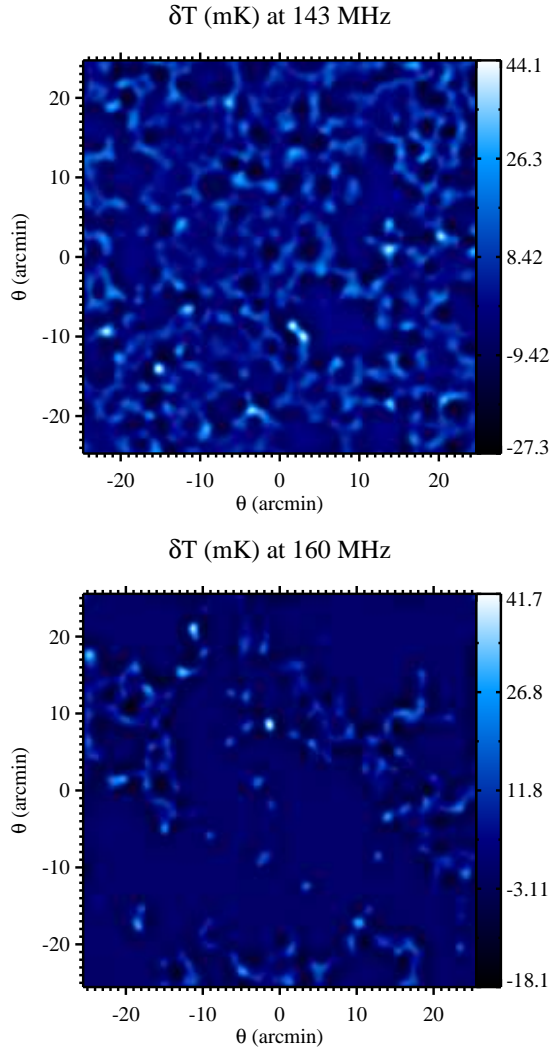


Fig. 3. Images of the redshifted 21cm signal at times of 50% (upper) and 90% (lower) ionization from f250_WMAP3. The signal has been convolved with a compensated Gaussian with a FWHM of $1'$ to simulate the effect of an interferometer beam.

$(1+z_1)/(1+z_3) \approx 1.4$, seems to apply. In particular an efficiency factor of 250 is capable of producing the measured WMAP optical depth for electron scattering, $\tau_{\text{es}} \approx 0.09$.

These results suggest that ground-based low frequency radio experiments will have a good chance to detect signals from the epoch of reionization if they are able to reach sensitivities of several 10s of mK.

References

- Alvarez, M. A., Shapiro, P. R., Ahn, K., & Iliev, I. T., 2006, ApJ, 644, L101
 Barkana, R. & Loeb, A., 2004, ApJ, 609, 474
 Ciardi, B. & Madau, P., 2003, ApJ, 596, 1
 Fan, X., et al., 2006, AJ, 132, 117
 Furlanetto, S., Oh, S. P., & Briggs, F., 2006, Physics Reports, 433, 181, (astro-ph/0608032)
 Furlanetto, S. R. & Briggs, F. H., 2004, New Astronomy Review, 48, 1039

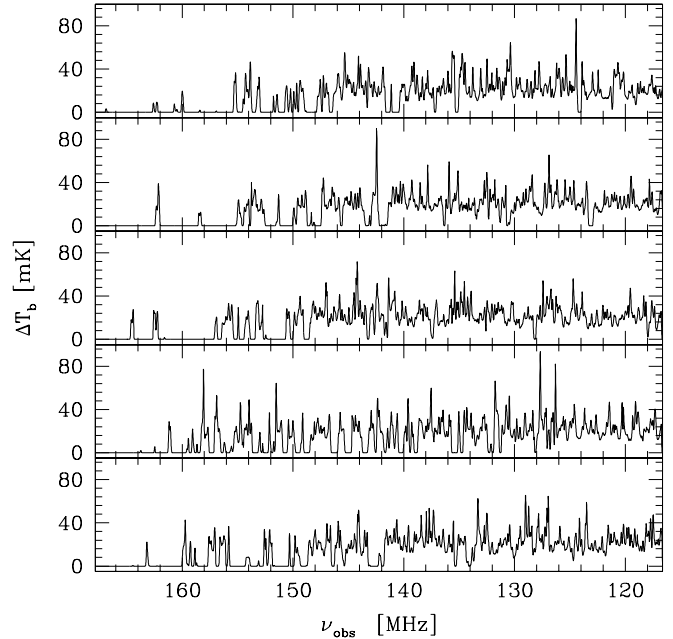


Fig. 4. Sample spectra of the redshifted 21cm signal from f250_WMAP3 along different lines of sight. The data are shown at the resolution of the simulation.

- Furlanetto, S. R., Zaldarriaga, M., & Hernquist, L., 2004, ApJ, 613, 1
 Iliev, I. T., et al., 2006a, MNRAS, 369, 1625
 Iliev, I. T., Mellema, G., Shapiro, P. R., & Pen, U.-L., 2007b, MNRAS, 376, 534
 Mellema, G., Iliev, I. T., Alvarez, M. A., & Shapiro, P. R., 2006a, New Astronomy, 11, 374
 Mellema, G., Iliev, I. T., Pen, U. L., & Shapiro, P. R., 2006b, MNRAS, 372, 679
 Merz, H., Pen, U.-L., & Trac, H. 2005, New Astronomy, 10, 393
 Spergel, D. N., et al., 2006, ApJS, 170, 377
 Spergel, D. N., et al., 2003, ApJS, 148, 175
 Springel, V., et al., 2005, Nature, 435, 629
 Wang, X. & Hu, W. 2006, ApJ, 643, 585
 Zhang, J., Hui, L., & Haiman, Z., 2006, MNRAS, 375, 2007